THE ASTROPHYSICAL JOURNAL, 317:112–120, 1987 June 1


# PRELIMINARY VLA LIMITS ON THE SUNYAEV-ZEL'DOVICH EFFECT IN ABELL 2218

R. B. PARTRIDGE
Haverford College
R. A. PERLEY
National Radio Astronomy Observatory,[1] Socorro, N.M.
N. MANDOLESI
TESRE/CNR, Bologna
AND
F. DELPINO
Dipartimento di Astronomia, Università di Bologna
*Received 1986 March 3; accepted 1986 November 11*

## ABSTRACT

In an attempt to apply radio interferometry or Fourier synthesis methods to the search for the Sunyaev-Zel'dovich effect, we used the Very Large Array of the National Radio Astronomy Observatory in its D configuration to map Abell cluster 2218 at $\lambda = 6$ cm. The phase center of the maps was offset from the cluster center to minimize systematic effects seen in other deep surveys. The presence of radio sources in the cluster and other, apparently instrumental, effects discussed here limited our sensitivity to the Sunyaev-Zel'dovich effect to $\Delta T \approx 0.7$ mK at an angular resolution of 60″–80″.

*Subject headings:* galaxies: clustering — galaxies: intergalactic medium — radio sources: galaxies

## I. INTRODUCTION

The Sunyaev-Zel'dovich effect (Sunyaev and Zel'dovich 1972) is a potentially important tool for determining the physical parameters of intergalactic gas (Birkinshaw, Gull, and Northover 1981; Boynton *et al.* 1982) and in addition offers a means of determining Hubble's constant independent of optical distance estimates (Gunn 1978; Silk and White 1978; Boynton and Murray 1978; Cavaliere, Danese, and De Zotti 1979). Unfortunately, measurements of the Sunyaev-Zel'dovich (SZ) effect in clusters of galaxies have produced few statistically significant and undisputed detections (see, for example, Rudnick 1978; Perrenod and Lada 1979; Lake and Partridge 1980; Birkinshaw, Gull, and Northover 1981; Birkinshaw, Gull, and Moffet 1981; Schallwich 1982; Lasenby and Davies 1983; Birkinshaw and Gull 1984; Birkinshaw, Gull, and Hardebeck 1984; Radford *et al.* 1986).

All the above measurements were made with filled-aperture radio telescopes. We report here a search for the SZ effect in one well-studied cluster of galaxies, Abell 2218, using interferometry or Fourier synthesis. This technique, presently at some cost in sensitivity, provides better angular resolution than filled-aperture observations (useful to find and eliminate discrete sources) and can produce a two-dimensional map of the SZ signal from the cluster. In addition, synthesis observations avoid some of the problems encountered in filled-aperture observations, such as side-lobe pick up, which we believe may be responsible for some of the disagreements among previous observations (e.g., Perrenod and Lada 1979; Lake and Partridge 1980; Birkinshaw and Gull 1984). On the other hand, synthesis measurements present problems of their own; our means of coping with some of them are explained in the following section.

For this preliminary study, we selected Abell 2218, in which detection of the SZ effect has been reported by three groups (Perrenod and Lada 1979; Schallwich 1982; Birkinshaw, Gull, and Hardebeck 1984). As the effective cluster and map center we used R.A. = $16^h35^m42^s$ and decl. = 66°20′00″ (1950).[2]

## II. OBSERVATIONAL TECHNIQUE

Our observations were made during the nights of 1983 June 9 and 10 at the Very Large Array (VLA) of the National Radio Astronomy Observatory in New Mexico. The VLA was in its D configuration with a maximum baseline spacing of ~1.1 km. At the frequency we employed, the synthesized beam of the array had a half-power full width of $\theta \approx 17''$. There were two independent channels, each of 50 MHz bandwidth, available in each of two circular polarizations. The channels were centered at 4835 and 4885 MHz. We used both channels and added polarizations to produce our final maps of total intensity (Stokes parameter $I$).

We observed the cluster for 13 hr. Data were averaged every 30 s. Observations of the cluster were interrupted every 30 minutes for calibration. As our primary calibrator, we used 3C 286, for which we took $S = 7.46$ Jy at 4835 MHz and $S = 7.41$ Jy at 4885 MHz in accord with the scale of Baars *et al.* (1977). As our phase calibrator, we used an unresolved source, 1634+628, near Abell 2218.

### a) *Offsetting the Phase Center*

Several VLA programs using long integration times have revealed both excess noise and variations in mean intensity at the phase center of VLA maps (Fomalont, Kellermann, and Wall 1984; Knoke *et al.* 1984). Some of this problem may be ascribed to antenna cross talk or to small offsets in some of the

[1] The National Radio Astronomy Observatory is operated by Associated Universities, Inc., under contract with the National Science Foundation.

[2] While this work was in preparation, we learned that M. Birkinshaw, S. Gull, and R. Padman, using a slightly different technique, had also used the VLA to search for the SZ effect in Abell 2218.

correlators. The variations in mean intensity display approximate circular symmetry about the phase center. We were therefore concerned that any such effect could mimic or mask an SZ signal if the phase center were located at the cluster center. (The peak amplitude of the concentric rings about the phase center was $\sim 15$ $\mu$Jy per synthesized beam in our map.) Therefore, we introduced a technique to displace the phase center 4′ in right ascension from the nominal cluster center, as shown in Figure 1. Although the phase center was offset, we arranged to have each antenna of the array pointing at the cluster center by applying a time-dependent 4′ pointing correction of opposite sign to each antenna. Thus the cluster was centered in the primary beam pattern of the antennas.[3] There was a small loss in sensitivity because it was necessary to introduce these pointing corrections in altitude and azimuth rather than directly in right ascension. We updated the pointing correction every 10 minutes; the maximum loss of sensitivity arising from this cause was 3% at the map center.

Our technique for offsetting the phase center of the map was

[3] A procedure to introduce such an offset of the phase center automatically has since been implemented at the VLA; in addition, the instrumental effect responsible for much of the problem at the phase center has now been identified by NRAO and will be corrected.

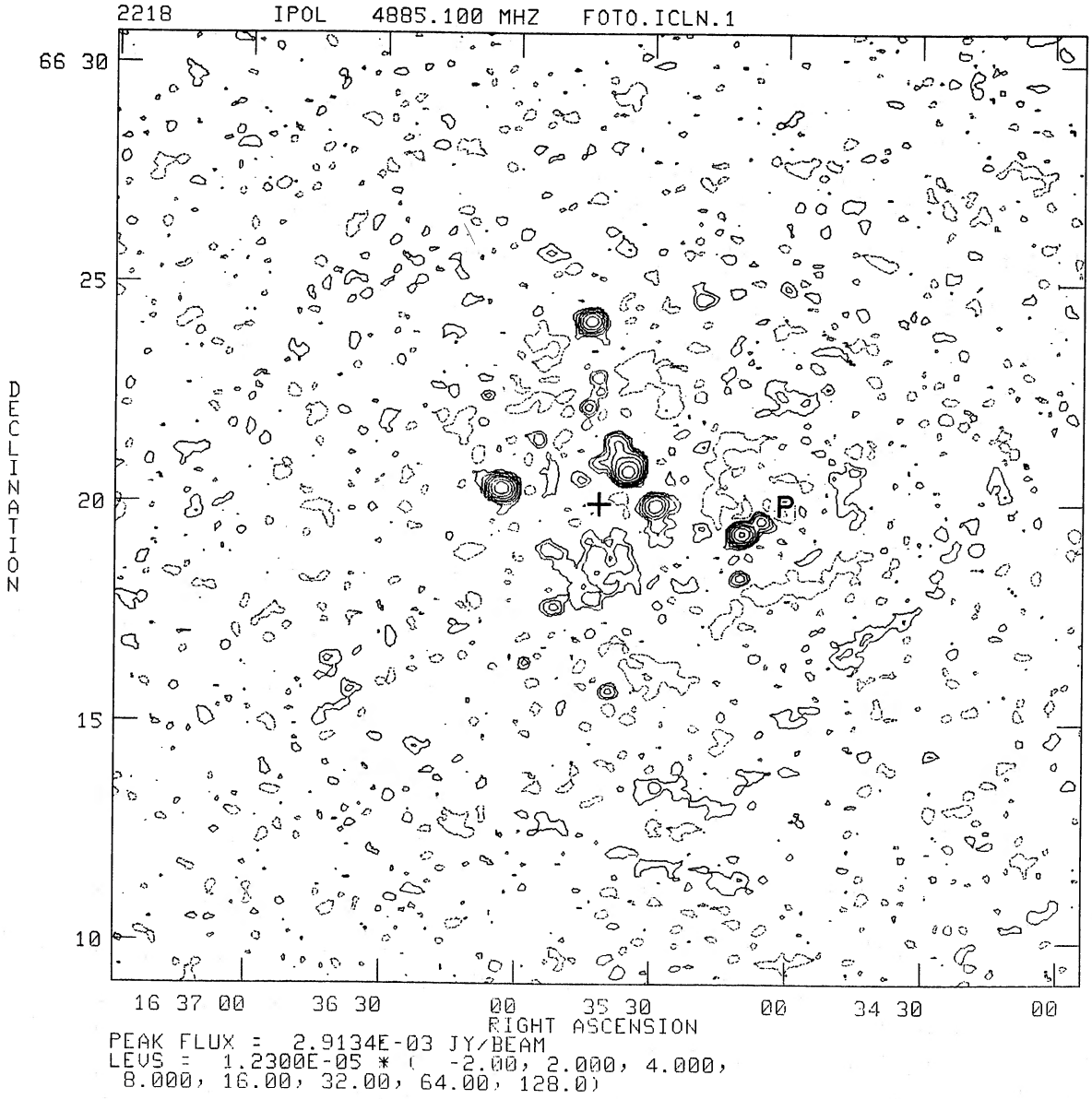


FIG. 1.—Central $21^2$ arcmin$^2$ region of the CLEANed 6 cm map of Abell cluster 2218 with radio sources *restored* after CLEANing. P marks the phase center, $\sim 4'$ west of the cluster center. The contour levels are at 24.6, 49.2, 98.4, 196.8, 393.6, 787.2 and 1574.4 $\mu$Jy per synthesized beam (*solid contours*) and $-24.6$ $\mu$Jy per beam (*dashed contours*). These levels correspond to 2, 4, ..., 128 and $-2$ times the rms noise of the map, respectively. The map has not been corrected for primary beam response.

TABLE 1

MAP PARAMETERS

| TAPER, $D_T$ (K$\lambda$) | NOISE LEVEL ($\mu$Jy per beam) | SYNTHESIZED BEAM PROPERTIES | |
|---|---|---|---|
| | | Half-Power Size | Solid Angle (arcsec$^2$) |
| None | 12.3 | 18".9 × 15".7 | 334 |
| 7.5 | 14.4 | 27.5 × 24.6 | 755 |
| 4.0 | 19 | 42.8 × 38.5 | 1846 |
| 2.5 | 25 | 60.9 × 55.4 | 3780 |
| 1.5 | 33 | 89.7 × 81.4 | 8150 |

checked 3 times during our run by observing calibration sources with both an offset beam and a centered beam. The observed change in flux density was unmeasurable for any of these tests.

## III. CONSTRUCTION OF MAPS

We first edited our data to remove interference spikes, results affected by noisy receivers and offset or biased correlators, and all measurements made when one antenna shadowed another. In all, ~9% of the visibility records were edited out. In the remaining data, only a few correlators (<1%) had closure errors >5°, and the mean closure error was 1°–2°.

We then used standard NRAO programs (Hjellming 1982) to construct maps of the cluster region 1024 cells on a side, with 5″ cells. In a departure from usual practice, we used natural rather than uniform weighting of the *u-v* plane data, since the former gives us a better signal-to-noise ratio. Both full-resolution and tapered maps were constructed; for the latter, a Gaussian weighting function of half-width $D_T$ at 30% of maximum was applied to the *u-v* plane data. The reduced weight of data at large distances from the center of the *u-v* plane broadened the synthesized beam (see Table 1).

### *a) Cleaning the Maps*

Our maps contained a number of discrete sources, a few of them radio sources lying within one cluster core radius of the center of the cluster we were studying (see Fig. 1). The brightest discrete sources had fluxes of 3–5 mJy and are discussed in a separate paper (Partridge, Hilldrup, and Ratner 1986). We CLEANed and removed both these sources *and* their associated sidelobes from the inner $512^2$ cells of our maps using standard NRAO deconvolution programs (Clark 1980). The maximum sidelobe amplitude was ~1%. The area CLEANed was $\sim 43^2$ arcmin$^2$, much larger than the primary beam pattern of the VLA antennas. Since we wished to CLEAN and remove radio sources without either affecting the noise statistics of the map or removing any possible contribution to the SZ signal, we first determined the number of CLEAN components which could be removed before the background noise level of the map was reached. In the case of the full-resolution, untapered map, we selected[4] 250 for this limit; at this level, the numbers of positive and of negative CLEAN components became roughly equal. In the case of tapered maps at lower resolution, fewer[4] CLEAN components were removed (e.g., 150 for $D_T = 2.5$ K$\lambda$ taper). We saw no tendency for the negative CLEAN components to clump preferentially near the cluster center, so we are not inadvertently subtracting out some of the SZ "dip" we seek by CLEANing and not restoring negative flux components to the map.

### *b) Zero-Spacing Flux Density*

Since the SZ signal may have an angular scale close to the primary power pattern of the antennas (say 2′–5′ compared to ~9′), an important component of its visibility will not be measured by the VLA. Under these conditions, we must rely on deconvolution to "fill in" the missing visibility data. An important component of the deconvolution process is the insertion of the correct zero-spacing flux density. To estimate this parameter, we summed the flux densities of all the discrete sources, including a small diffuse patch ~2′ south of the cluster center we used. This value was then corrected by ~0.2 mJy for the (negative) flux density expected from the SZ signal itself. The result was 14 mJy. Tests were run with different values (12–16 mJy) for the zero-spacing flux density with no significant differences in the final maps. In the deconvolution process, we applied the zero-spacing flux with a weight determined by estimating the number of missing (unsampled) cells at the center of the *u-v* plane. Since this estimate is not rigorous, tests were run with different weights as well, with no significant differences in the final maps.

The results of all these steps was an untapered, full-resolution map with rms noise in regions away from discrete sources of 12.3 $\mu$Jy per synthesized beam area. This value was within 10% of the theoretical system noise of the instrument. The corresponding noise levels for tapered maps are given in Table 1.

Though the discrete sources were CLEANed and removed, it is important to recall that even carefully CLEANed maps will contain some residual flux at the locations of strong discrete sources. We attempt to cope with this problem in two ways.

### *c) Further Attempts to Remove Sources*

Our first technique to deal with residual flux from sources was to make maps with a two-step CLEANing process which emphasized removing flux in the vicinity of discrete sources. The first step was to locate and remove CLEAN components only from small polyhedral boxes centered on the sources. The number of boxes used depended on the resolution of the map. For the full-resolution, untapered map, 11 boxes covering the 18 brightest sources were used (see Fig. 2 [Pl. 1]); for lower resolution, tapered maps, fewer boxes were needed. Typically, 50–100 CLEAN components were removed, thereby CLEANing these small regions thoroughly. The second step in this two-step process was to CLEAN the remainder of the map, again not restoring the sources.

Our second technique was to blank out the areas of the CLEANed map included in the small polyhedral boxes centered on sources, thereby removing these regions from the map altogether. Unless otherwise noted, the results we present will be drawn from maps made with regions around sources removed from the maps by this technique. (As we show in § V*b* below, removing these regions had an insignificant effect on our final results.)

## IV. CORRECTIONS TO THE MEASURED FLUX DENSITIES

We next took account of the primary beam response of the individual antennas of the array, which introduces a dependence of the observed flux densities on radial distance from the *cluster center*, which coincided with the pointing direction of

[4] But see § V*b* below.

PLATE 1

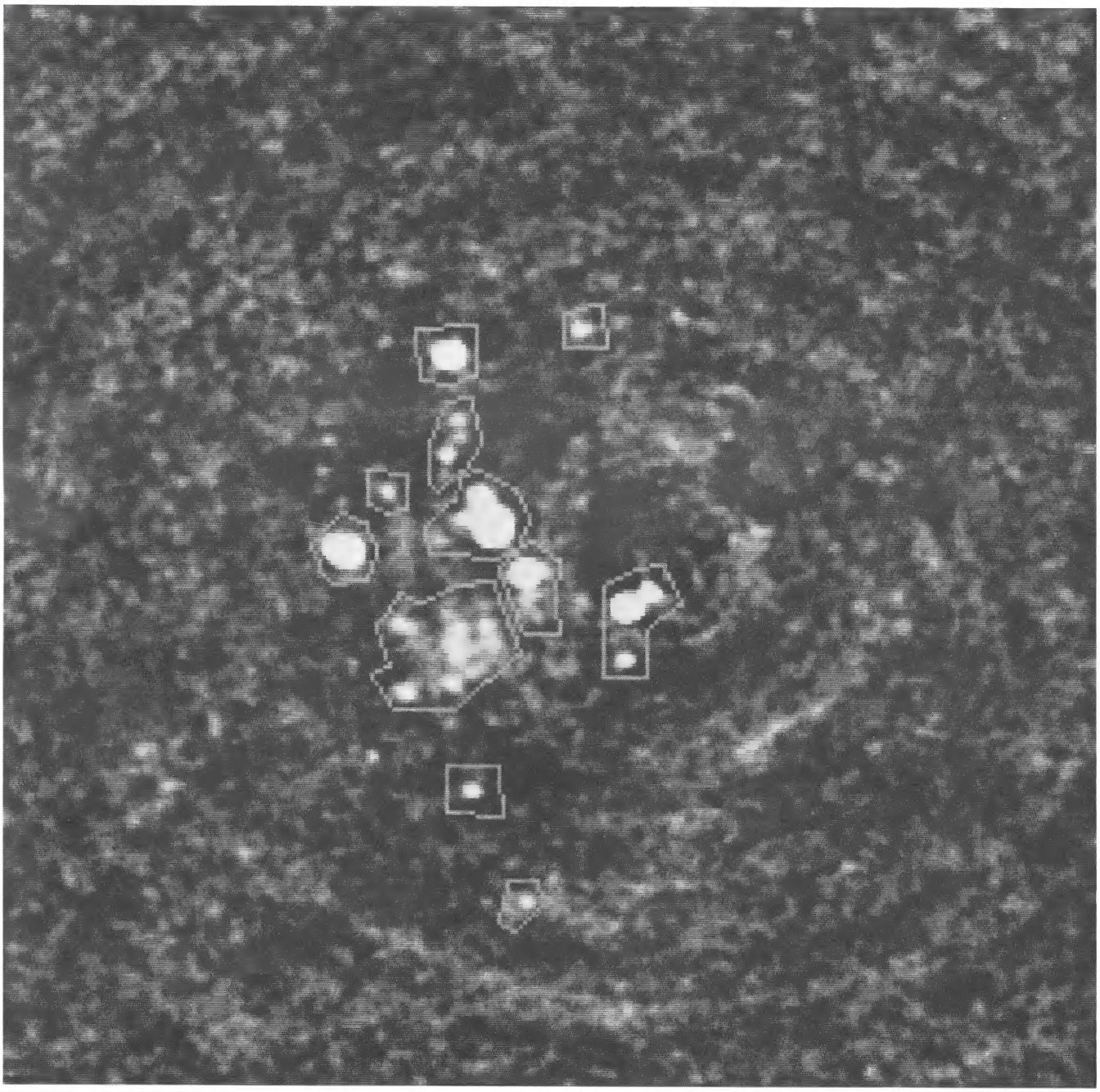

FIG. 2.—Location of the polyhedral "boxes" placed around discrete sources in our untapered map. For most of our analysis, these 11 regions were excised from the map and excluded.

317

PARTRIDGE *et al.* (*see* page 114)

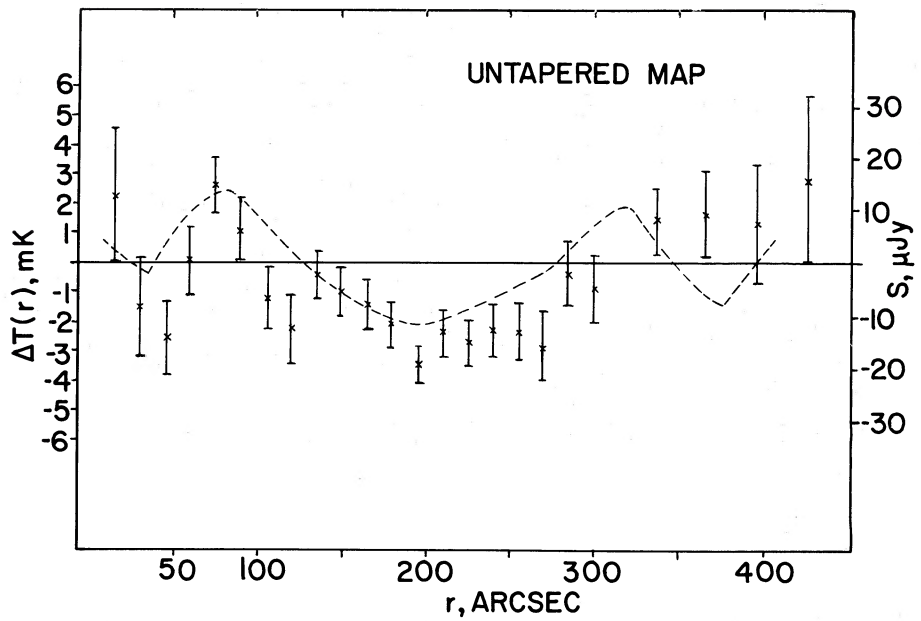


FIG. 3.—Radial profiles of the sky brightness temperature as a function of the distance from the cluster center, $r$, for the untapered full-resolution maps: points with associated 1 $\sigma$ internal error bars are shown for a map with boxes around the locations of discrete sources removed; dashed curve indicates similar results for a map with no boxes removed.

the antennas. We multiply all our measured flux densities by a factor equal to the inverse of the primary beam power pattern, given by

$$P^{-1}(r) = 0.9920 + 2.3518 \times 10^{-2} r^2 + 2.1281 \times 10^{-3} r^4 - 6.9992 \times 10^{-5} r^6 + 1.2390 \times 10^{-6} r^8$$

for our central frequency of 4860 MHz (from an updated version of Napier and Rots 1982). Here, $r$ is radial distance from the pointing direction, expressed in arcminutes.

Also, although they had a negligible effect on our results, we made the corrections to our measured flux densities required for the integrating time and the band width employed (see Chap. 2 of Hjellming 1982). These corrections depend on the radial distance from the *phase center* of the map and were $< 5\%$ for point sources within 8′ of the phase center.

## V. SEARCH FOR RADIAL FLUX DEPENDENCE

We then examined these corrected values for any dependence on radial distance from the cluster center by averaging the flux density $S$ in annuli of equal increments in radius, centered on the cluster. For the inner 5′ of the maps, annuli with radial increments of 15″ were used; for larger values of the radial distance, $\Delta r = 30''$. The results of this analysis for the untapered map with the two step CLEANing process are shown in Figure 3 and presented numerically in Table 2. The conversion of flux per synthesized beam, $S$, to brightness temperature is

$$T = \frac{S\lambda^2}{2k\Omega}, \quad (1)$$

where $\Omega$ is the solid angle of the synthesized beam as given in Table 1. We computed $\Omega$ by assuming a Gaussian beam profile, a good approximation for these very fully deconvolved maps.

### a) *Features of the Radial Plot*

The slow decrease in size of the error bars in Figure 3 as $r$ rises to $\sim 200''$ results from the increase in the area of the annular rings, and hence the number of cells, over which the

TABLE 2

RADIAL PROFILES OF SKY BRIGHTNESS TEMPERATURE[a]

| | NOMINAL CLUSTER CENTER | | | BIRKINSHAW *et al.* 1984 CENTER[c] |
|---|---|---|---|---|
| $r$ | Untapered | 2.5 K$\lambda$ Taper[b] | 1.5 K$\lambda$ Taper[b] | |
| 15″ ..... | +2.3 ± 2.3 | ... | ... | ... |
| 30 ..... | −1.5 ± 1.7 | +0.21 ± 0.30 | +0.53 ± 0.14 | ... |
| 45 ..... | −2.6 ± 1.2 | ... | ... | +2.9 ± 2.0 |
| 60 ..... | +0 ± 1.2 | +0.32 ± 0.55 | +0.43 ± 0.28 | −0.4 ± 1.5 |
| 75 ..... | +2.6 ± 0.9 | ... | ... | +0 ± 1.1 |
| 90 ..... | +1.0 ± 1.2 | +0.30 ± 0.38 | +0.38 ± 0.26 | +0.4 ± 1.2 |
| 105 ..... | −1.1 ± 1.0 | ... | ... | −0.5 ± 0.9 |
| 120 ..... | −2.2 ± 1.2 | −0.10 ± 0.50 | +0.13 ± 0.39 | −0.9 ± 0.8 |
| 135 ..... | −0.4 ± 0.8 | ... | ... | −1.0 ± 0.8 |
| 150 ..... | −1.0 ± 0.8 | −0.38 ± 0.35 | −0.17 ± 0.33 | −2.2 ± 0.9 |
| 165 ..... | −1.4 ± 0.9 | ... | ... | −2.9 ± 0.8 |
| 180 ..... | −2.1 ± 0.8 | −0.67 ± 0.29 | −0.44 ± 0.29 | −2.4 ± 0.7 |
| 195 ..... | −3.4 ± 0.6 | ... | ... | −1.8 ± 0.7 |
| 210 ..... | −2.3 ± 0.8 | −0.89 ± 0.24 | −0.68 ± 0.23 | −2.1 ± 0.8 |
| 225 ..... | −2.7 ± 0.8 | ... | ... | −1.9 ± 0.8 |
| 240 ..... | −2.3 ± 0.9 | −0.80 ± 0.37 | −0.72 ± 0.34 | −1.8 ± 0.9 |
| 255 ..... | −2.3 ± 0.9 | ... | ... | −2.5 ± 0.9 |
| 270 ..... | −2.9 ± 1.0 | −0.82 ± 0.45 | −0.63 ± 0.44 | −1.8 ± 1.0 |
| 285 ..... | −3.3 ± 1.1 | ... | ... | −2.1 ± 1.1 |
| 300 ..... | −0.8 ± 1.2 | −0.52 ± 0.46 | −0.34 ± 0.50 | −1.7 ± 1.3 |
| 330 ..... | +1.4 ± 1.0 | +0.21 ± 0.63 | +0.12 ± 0.63 | +1.3 ± 1.1 |
| 360 ..... | +1.6 ± 1.4 | +0.44 ± 0.83 | +0.62 ± 0.85 | +3.6 ± 1.5 |
| 390 ..... | +1.3 ± 2.0 | +0.42 ± 1.33 | +0.87 ± 1.21 | +2.6 ± 1.9 |
| 420 ..... | +2.9 ± 2.9 | +1.31 ± 1.92 | +1.27 ± 1.80 | +3.2 ± 2.9 |

[a] Brightness temperature and 1 $\sigma$ error bars, expressed in mK.

[b] Note that the tabulated values are not fully independent, since the synthesized beam width is larger than the thickness of the annulus $\Delta r$.

[c] Cluster center as given by Birkinshaw *et al.* 1984: R.A. = $16^h35^m37^s$, decl. = 66°18′30″.

flux density was averaged. As $r$ increases beyond $\sim 200''$, the errors begin to increase again because the correction for the primary beam response effectively multiplies the instrumental noise by a factor $P^{-1}(r) > 1$.

The most striking features in Figure 3 are the apparent oscillations, with troughs at values of $r \approx 50''$ and $r \approx 200''$, and a weak peak at $r \approx 80''$. These features are produced by patches of high and low flux density in our CLEANed map—some are displayed in Figure 4, which outlines regions of *negative* flux density. The instrumental rings concentric with the phase center are also marginally visible in Figure 4. Note that they are offset from the cluster center. More striking are the six or seven regions of negative flux density approximately centered on the cluster position and 3′–5′ from it. These patches, we believe, are responsible for the trough in our radial plot. Note that comparable patches appear all over the region mapped, including the edges of the map where the primary beam response is small ($< 0.25$). This fact suggests the patches are instrumental in origin and *not* real features on the sky.

### b) *Investigation of Patches of High and Low Flux Density*

In any case, this apparently instrumental effect sets the fundamental limit on the accuracy of this search for the SZ effect. Making radial plots similar to Figure 3, but centered at random places on our untapered map, suggests that spurious oscillations of amplitude up to 2 mK are possible for the untapered, full resolution, map. Given the importance of this effect, we made a number of trials to track down its origin.

First, since some of the patches of emission are found near the positions of discrete sources, we investigated the effects of the residual flux from sources left by the CLEANing process. We did so by comparing radial plots of brightness temperature

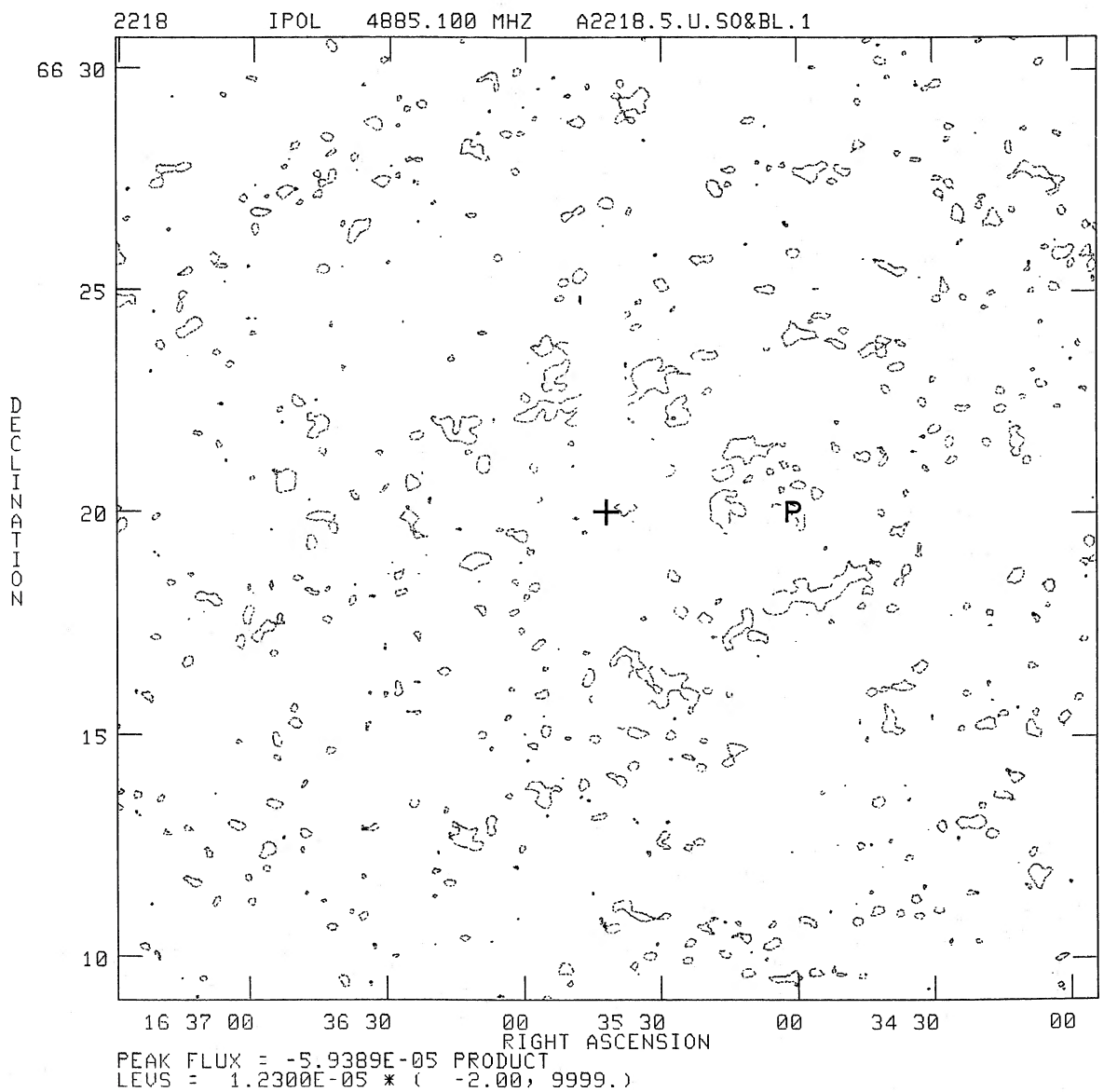


FIG. 4.—Central $21^2$ arcmin$^2$ region of the CLEANed 6 cm map with sources *not restored* after CLEANing. Here, a single contour at $-24.6$ μJy per beam is used to outline the patches of emission we believe are responsible for the oscillatory behavior of our radial plots. Note especially those patches lying $\sim 3'$–$5'$ from the cluster center we used (marked by a cross); these patches may cause the "trough" observed in Fig. 3. P marks the phase center. The map has not been corrected for primary beam response.

made from CLEANed untapered maps (1) with regions inside boxes around each source *excised* (see § III*c*), and (2) with those regions *included*. The results are shown in Figure 3; the two plots show the same qualitative features, including oscillations. Although this test did not show that residual flux from the CLEANed sources contributed significantly to the apparently instrumental oscillations in our plots of $\Delta T(r)$, we chose to work with maps with the regions around sources excised. The results we report below are based on the analysis of maps with those regions omitted (see § III*c* and Fig. 2).

We also examined the effect on plots such as Figure 3 of discrete sources weaker than those "boxed" and omitted from the map. Correcting for the presence of these weaker sources would have lowered $\Delta T$ by about one third of the 1 $\sigma$ error bars in several radial bins of Figure 3 ($r$ = 15″, 75″, 105″ and 180″, for instance). Thus the flux from these weak sources does not qualitatively affect our radial plots, or account for the oscillations observed in them.

In an attempt to see if the CLEANing process had any effect on the patches, we varied the number of CLEAN components (up to 1000). We saw no change.

As noted in § III*b* above, we varied both the amplitude and the weighting of the zero-spacing flux added to the map; no discernible change resulted.

We used NRAO's standard programs in AIPS to self-calibrate the data in phase only. Despite the faintness of the sources in the field (the brightest had a 6 cm flux density of 5 mJy), self-calibration was successful. There was no significant improvement in the properties of the map. This is not surprising because the intrinsic phase stability is not the limiting factor in the sensitivity of our work.

### c) *Use of Tapered Maps*

Since we were not able to solve this apparently instrumental problem in our data, we sought instead to dilute it by working with tapered maps, for which the synthesized beam solid angle is larger, and the resulting sensitivity to the SZ effect greater.

As Table 1 shows, the rms noise in the maps increases with the degree of taper since more and more of the *u-v* plane data is effectively excluded by the tapering. We also find that the amplitude of the oscillations increases, when the amplitude is expressed in units of flux density per synthesized beam (compare the right-hand vertical axes of Figs. 3 and 6). That increase in amplitude suggests that patchy regions which we believe produce the oscillations are produced primarily by the shortest baselines of the VLA array. Their angular scale of 1′–2′ also supports that view. Nevertheless, tapering increases the relative sensitivity to SZ signals larger than the beam size, since brightness temperature is inversely proportional to the solid angle of the synthesized beam (eq. [1]). By tapering to 1.5 K$\lambda$, we reduce the amplitude of the oscillations in brightness temperature to $\Delta T \approx 0.7$ mK. The numerical results for maps with several degrees of taper are displayed in Figures 5 and 6 and in Table 2. For the more heavily tapered, lower resolution maps, larger radial increments were used, to keep $\Delta r$ comparable to the resolution.

### d) *Additional Radial Plots*

Finally, we made a series of radial plots centered on the co-ordinates used by Birkinshaw, Gull, and Hardebeck (1984) and Schallwich (1982) for the cluster center: R.A. = $16^h35^m37^s$ and decl. = 66°18′30″ (~1′.5 south of our nominal cluster center). These results appear in the fifth column of Table 2 and in Figure 7. The gross features of these plots are again explained, we believe, by the patchy regions referred to in § V*a* above and shown in Figure 4.

## VI. COMPARISON WITH MODELS OF THE SUNYAEV-ZEL'DOVICH EFFECT

The results displayed in Figures 3 and 5–7 show no significant evidence for a SZ "dip" at either the cluster center we

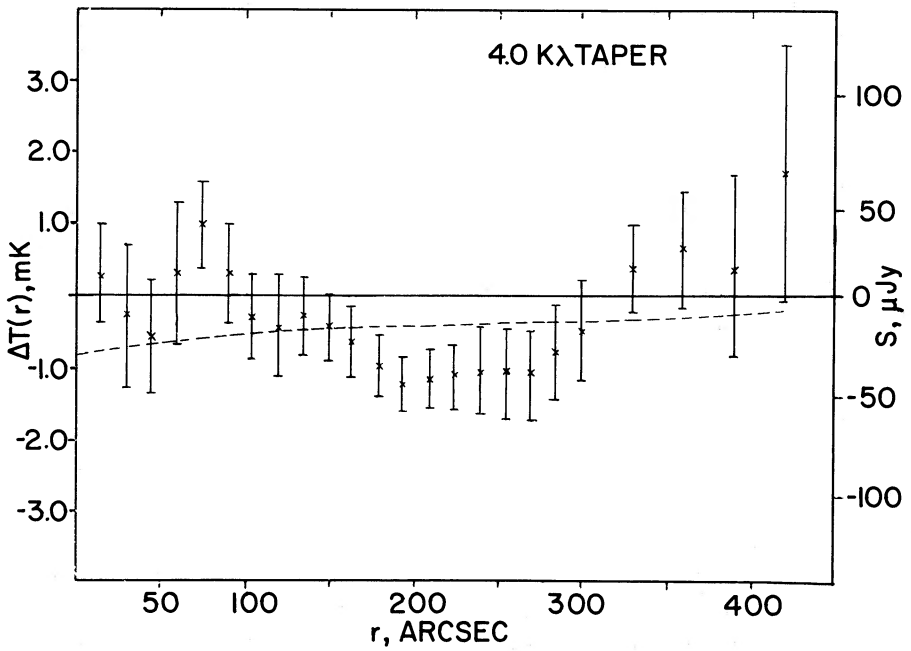


FIG. 5.—Radial plot for a tapered map, with $D_T$ = 4.0 K$\lambda$ and a synthesized beam full-width of ~40″ (with boxes removed). The plotted points are not fully independent since the beam width is greater than the interval between samples $\Delta r$. (*dashed curve*) Model profile as given by eq. (2) for $\Delta T_0$, the central decrement, equal to −0.8 mK.

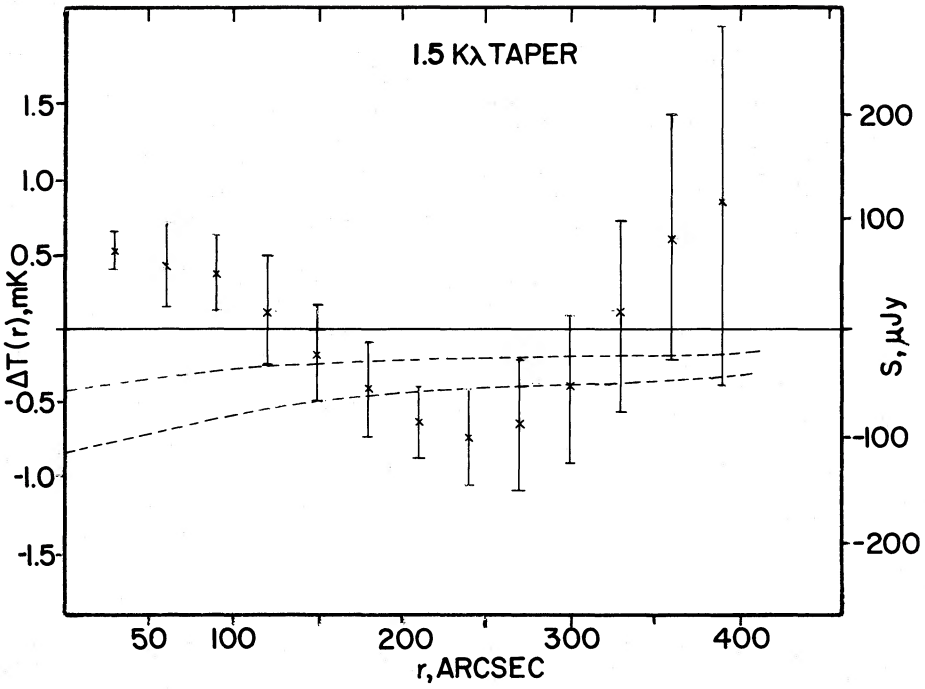


FIG. 6.—Radial plot for a tapered map, with $D_T = 1.5\ K\lambda$ and a synthesized beam width of $\sim 85''$ (with boxes removed). Again the beam width exceeds $\Delta r$, so the points are not fully independent. (*dashed curve*) Model profiles as given by eq. (2) for $\Delta T_0 = -0.4$ and $-0.8$ mK.

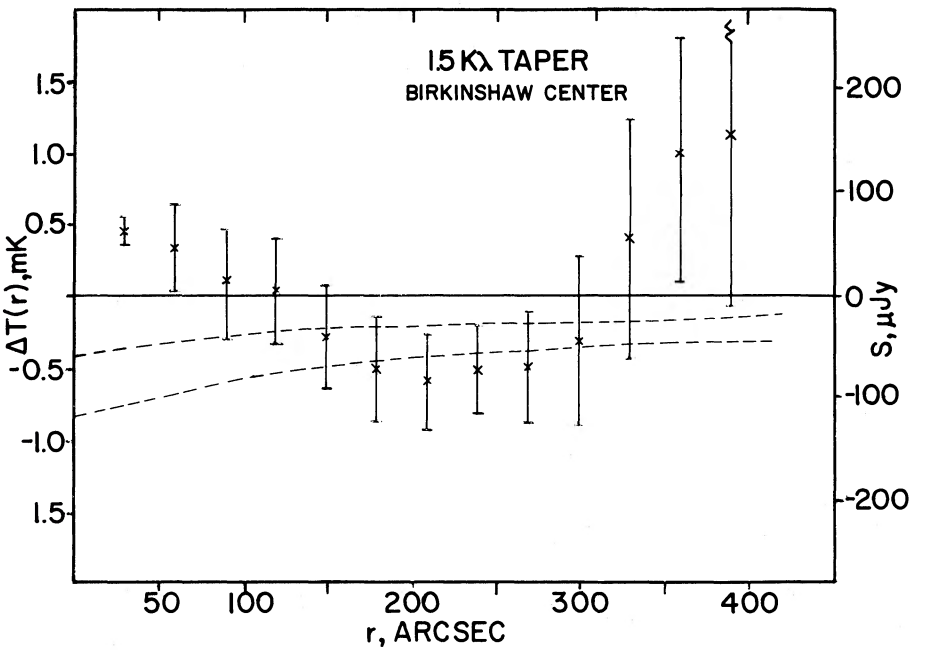


FIG. 7.—Radial plot for a tapered map, with $D_T = 1.5\ K\lambda$, centered on the cluster position as given by Birkinshaw *et al.* (1984), $\sim 1'.5$ south of our nominal cluster center. Again the beam width exceeds $\Delta r$, so the points are not fully independent. (*dashed curves*) Model profiles as given by eq. (2) for $\Delta T_0 = -0.8$ mK. Excluding the data inside the boxes removed all data for $r \leq 30''$.

used or the center used by Birkinshaw, Gull, and Hardebeck (1984). Indeed, most of the radial plots indicate an excess of flux near the cluster center, even with regions around the discrete sources removed from the map.

To estimate the approximate limits placed by our observations on the magnitude of the SZ effect in Abell 2218, we compared our results with the model profile for the SZ effect adopted by Birkinshaw, Gull, and Hardebeck (1984):

$$\Delta T(r) = \Delta T_0[1 + (r^2/r_c^2)]^{-1/4}, \quad (2)$$

where $r_c$ is the cluster core radius as determined from X-ray observations—$r_c = 58''$ for Abell 2218 (Boynton *et al.* 1982). This model profile applies if we assume the intergalactic plasma in the cluster is isothermal and has spherical symmetry. We note that other assumptions about the state and distribution of the plasma can result in models with less gradual radial dependence, i.e., generally smaller angular scale. For their model, Birkinshaw, Gull, and Hardebeck (1984) report values of the central decrement $\Delta T_0 = -0.4$ to $-0.8$ mK, depending on the assumption made about systematic offsets in their observations. The dashed curves in Figures 5–7 represent the profile given in equation (2) evaluated with $\Delta T_0 = -0.4$ and $-0.8$ mK. No attempt was made to convolve the theoretical profile with our beam pattern. Our data are obviously in poor agreement with the radial profile predicted by this model.

### *a) Effect of Residual Diffuse Emission from the Cluster*

While we eliminated the effect of the 18 brightest discrete sources by removing regions around them from our maps (as noted in § V), there remains the possibility that a weak, extended radio source in Abell 2218 could have obscured the SZ effect we sought. Indeed, both Schallwich (1982) and Birkinshaw (1985) report evidence for a diffuse halo radio source centered at $16^h35^m42^s$ and $+66°18'25''$ with an extent of an arcminute or more (this region of enhanced emission is also apparent in Fig. 1). Let us ask how much residual flux density from such a source would bring the results for tapered maps shown in Figures 6 and 7 into agreement with a SZ decrement of $\Delta T_0 = -0.8$ mK. If we assume that the extent of the radio source is a fraction $f$ of our synthesized beam solid angle of $\Omega = 8150$ arcsec$^2$, then the residual flux density required to explain the results we obtain given a real central decrement of $-0.8$ mK is $S \approx 180\ \mu$Jy for $f < 1$ and $S \approx 180f\ \mu$Jy for $f \gg 1$.

Can a diffuse source contribute this much flux to our map? The work of Birkinshaw (1985) suggests $f \approx 1$ and a total flux density of $\sim 600\ \mu$Jy at $\lambda = 6$ cm for the diffuse source near the center of the cluster used by Birkinshaw, Gull, and Hardebeck (1984). On the other hand, much of this 600 $\mu$Jy diffuse source has been removed from our map by the technique described in § III*c* above (it is excluded by the largest, least regular, box shown in Fig. 2). Our estimate of the flux density thus excised from the map in the vicinity of this source is $900 \pm 200\ \mu$Jy. Thus a residual flux density of $\sim 180\ \mu$Jy is only marginally possible but may help explain why we see excess flux rather than a SZ decrement.

### *b) Conclusions*

Both the presence of this diffuse source and the instrumental effects described in § V limit the accuracy of this preliminary attempt to map the SZ effect to $\sim 0.7$ mK. Our results are probably not inconsistent with the 0.4–0.8 mK SZ signal reported by Birkinshaw, Gull, and Hardebeck (1984) on the basis of their filled-aperture observations at $\lambda = 1.5$ cm but also do not provide useful supporting evidence for it. Our measurements do conflict with much larger values of the SZ "dip" reported earlier by Perrenod and Lada (1979), Birkinshaw, Gull, and Northover (1981), and Schallwich (1982).

As noted in § I, the use of Fourier synthesis techniques in searches for the SZ effect has some advantages over filled-aperture observations. There are also drawbacks, however, and our work has revealed some of them. The presence of concentric rings around the phase center is an instrumental effect at the VLA, and we understand that hardware changes may soon largely eliminate it. It is not clear whether the large diffuse patches of positive and negative flux shown in Figure 4 and which we believe are responsible for the oscillatory behavior in our radial plots are a fundamental instrumental effect, like the concentric rings discussed in § II*a*, or are related to some other property of the map. If these systematic errors can be eliminated, the VLA is capable of detecting and mapping the SZ effect at the 0.2 mK level in a single $\sim 12$ hr observing run such as this one.

The presence of a diffuse source or sources near the cluster center will cause problems for any attempt to measure the SZ signal in Abell 2218, whether filled aperture or synthesis observations are employed. It may be necessary to make observations at much shorter wavelengths, where the flux from a halo source is likely to be less. Clusters other than Abell 2218 may be more suitable targets for future attempts to measure the SZ effect. In particular, it may prove advantageous to select a cluster at a larger distance, in order to get a better match between the angular scale of the SZ profile and the synthesized beam of the VLA. This is especially true if observations at a shorter wavelength (e.g., 2 cm) are planned. Together with other colleagues, we are planning further observations of the SZ effect along the lines suggested by this preliminary work.

The suggestion to offset the phase center from the pointing direction of the antennas was made to us by Ed Fomalont of NRAO. We wish to thank Roger Foster of Haverford for his assistance in various phases of the data analysis. We had several helpful conversations with T. J. Cornwell at NRAO, New Mexico. The paper was substantially improved by the comments and criticisms of an anonymous referee. This work was supported in part by a National Science Foundation grant AST 80-0737 to Haverford College and by the Consiglio Nazionale delle Ricerche of Italy. Final revisions of this paper were made while two of us, N. M. and R. B. P., were guests of the Institute of Astronomy in Cambridge, and we thank Donald Lynden-Bell and Martin Rees for their hospitality there.

## REFERENCES

Baars, J. W. M., Genzel, R., Pauliny-Toth, I. I. K., and Witzel, A. 1977, *Astr. Ap.*, **61**, 99.
Birkinshaw, M. 1985, preprint.
Birkinshaw, M., and Gull, S. F. 1984, *M.N.R.A.S.*, **206**, 359.
Birkinshaw, M., Gull, S. F., and Hardebeck, H. 1984, *Nature*, **309**, 34.
Birkinshaw, M., Gull, S. F., and Moffet, A. T. 1981, *Ap. J. (Letters)*, **251**, L69.
Birkinshaw, M., Gull, S. F., and Northover, K. J. E. 1981, *M.N.R.A.S.*, **197**, 571.
Boynton, P. E., and Murray, S. S. 1978, *HEAO-B* Guest Observer Proposal.
Boynton, P. E., Radford, S. J. E., Schommer, R. A., and Murray, S. S. 1982, *Ap. J.*, **257**, 473.
Cavaliere, A., Danese, L., and De Zotti, G. 1979, *Astr. Ap.*, **75**, 322.
Clark, B. G. 1980, *Astr. Ap.*, **89**, 377.
Fomalont, E. B., Kellermann, K. I., and Wall, J. V. 1984, *Ap. J. (Letters)*, **277**, L23.

Gunn, J. E. 1978, in *Observational Cosmology*, ed. A. Maeder, L. Martinet, and G. Tammann (Geneva: Geneva Observatory), p. 3.
Hjellming, R. M. 1982, *An Introduction to the NRAO Very Large Array* (Socorro, N.M.: NRAO).
Knoke, J. E., Partridge, R. B., Ratner, M. I., and Shapiro, I. I. 1984, *Ap. J.*, **284**, 479.
Lake, G., and Partridge, R. B. 1980, *Ap. J.*, **237**, 378.
Lasenby, A. N., and Davies, R. 1983, *M.N.R.A.S.*, **203**, 1137.
Napier, P. J., and Rots, A. H. 1982, *VLA Test Memorandum 134* (Socorro, N.M.: NRAO).
Partridge, R. B., Hilldrup, K. S., and Ratner, M. I. 1986, *Ap. J.*, **308**, 46.
Perrenod, S. C., and Lada, C. J. 1979, *Ap. J. (Letters)*, **234**, L173.
Radford, S. J. E., Boynton, P. E., Ulich, B. L., Partridge, R. B., Schommer, R. A., Stark, A. A., Wilson, R. W., and Murray, S. A. 1986, *Ap. J.*, **300**, 159.
Rudnick, L. 1978, *Ap. J.*, **223**, 37.
Schallwich, D. 1982, Ph.D. thesis, University of Bochum, FRG.
Silk, J., and White, S. D. M. 1978, *Ap. J. (Letters)*, **226**, L103.
Sunyaev, R. A., and Zel'dovich, Ya. B. 1972, *Comments Ap. Space Phys.*, **4**, 173.

F. DELPINO: Dipartimento di Astronomia, Università di Bologna, 40126 Bologna, Italy

N. MANDOLESI: TESRE/CNR, Via de Castagnoli 1, 40126 Bologna, Italy

R. B. PARTRIDGE: Haverford College, Haverford, PA 19041

R. A. PERLEY: NRAO Post Office Box 0, Socorro, NM 87801